



Deposited via The University of Leeds.

White Rose Research Online URL for this paper:

<https://eprints.whiterose.ac.uk/id/eprint/80859/>

Version: Accepted Version

Article:

Bryant, M, Farrar, R, Freeman, R et al. (2014) Galvanically enhanced fretting-crevice corrosion of cemented femoral stems. *Journal of the Mechanical Behavior of Biomedical Materials*, 40. pp. 275-286. ISSN: 1751-6161

<https://doi.org/10.1016/j.jmbbm.2014.08.021>

© 2014, Elsevier. Licensed under the Creative Commons Attribution-NonCommercial-NoDerivatives 4.0 International <http://creativecommons.org/licenses/by-nc-nd/4.0/>

Reuse

Items deposited in White Rose Research Online are protected by copyright, with all rights reserved unless indicated otherwise. They may be downloaded and/or printed for private study, or other acts as permitted by national copyright laws. The publisher or other rights holders may allow further reproduction and re-use of the full text version. This is indicated by the licence information on the White Rose Research Online record for the item.

Takedown

If you consider content in White Rose Research Online to be in breach of UK law, please notify us by emailing eprints@whiterose.ac.uk including the URL of the record and the reason for the withdrawal request.

Galvanically Enhanced Fretting-Crevice Corrosion of Cemented Femoral Stems

M.Bryant^a, R. Farrar^b, R. Freeman^b, K. Brummitt^b, J. Nolan^c, A. Neville^a

a – Institute of Functional Surfaces (iFS), School of Mechanical Engineering, University of Leeds, Leeds, LS2 9JT, United Kingdom .

b – DePuy International, Millshaw Park Lane, Leeds, LS11 0BG. United Kingdom.

c – Norfolk and Norwich University Hospital, Norwich, United Kingdom.

ABSTRACT

The Ultima TPS MoM THR was designed and developed as a 2nd generation MoM THR specifically aimed at younger more active patients due to the anticipated low wear rates and increased longevity of MoM THRs. In 2010, published clinical data highlighted the early failure of the Ultima TPS MoM due to fretting-crevice corrosion at the stem-cement interface. Since 2010 similar observations have been reported by other clinical centres implicating competitor products as well as the Ultima TPS MoM THR. In an attempt to replicate the electrochemical reaction and interactions established across MoM THR systems, fretting-crevice corrosion tests subjected to galvanic coupling were conducted. Galvanic coupling was seen to significantly increase the rates of corrosion under static and dynamic conditions. This was due to the large potential differences developed across the system between active and passive areas, increasing the rates of corrosion and metallic ion release from the stem-cement interface.

1. Introduction

Joint replacements have been a medical intervention practised since the late nineteenth century (Reynolds and Tansey, 2006). However it has only been since the 1950's it has become a long term solution to arthritic and congenital diseased joints since the 1950's due to the advances in both fixation techniques and implant design made by Sir John Charnley. The orthopaedic industries have made many advances since and Total Hip Arthroplasty (THA) is now widely accepted as being a successful surgical procedure with results from the National Joint Registry supporting this (National Joint Registry, 2012). THAs are commonly used to treat arthritis or severe joint damage. Osteoarthritis of the hip joint is a painful and debilitating condition, estimated to affect 8 million people in the United Kingdom and 27 million in the United States (National Joint Registry, 2012; World Health Organisation, 2003). Different

treatments exist to treat the condition but to date the most effective method of alleviating pain and restoring motion is THA.

MoM Total Hip Replacements (THR) have the longest clinical history of any of the bearing combinations with the first generation of MoM THR being designed and developed by Philip Wiles in 1938 (A.Santavirta et al., 2003). However these implants were largely unsuccessful due to the poor quality of material which was primarily stainless steel, poor manufacture and lack of inadequate fixation within the body (Reynolds and Tansey, 2006). MoM THR's regained popularity in the last 10 years due to improved manufacturing methods and decreased wear rates (Fisher et al., 2006). Retrieval studies indicate that well-functioning MoM THRs produce minimal wear debris and the surrounding tissues appear to have less inflammation compared with typical histiocyte-dominated tissue response to polyethylene debris (Jacobs et al., 1998). However in the recent years the amount of revisions has increased due to the Adverse Reaction to Metal Debris (ARMD).

The Ultima TPS™ was introduced in 1997 as triple tapered, highly polished cemented femoral stem. The Ultima TPS™ was primarily used with a MoM bearing typically coupled with a 28mm 10/12 taper low CoCrMo Ultima femoral head, 28mm high CoCrMo Ultima acetabular liner and a Ti-6Al-4V cementless acetabular shell that ranged from 48mm – 68mm in size. Polished tapered femoral stems generally have a good survivorship with revision rates of 2.8% at 7 years after operation being seen for commonly cemented stainless steel devices (Purbach et al., 2009). Similar figures have been presented for CoCrMo polished demonstrating revision rates of 4.1% 10 years postoperative (Burston et al., 2012). However recent studies have highlighted the importance of wear and corrosion, known as *tribocorrosion*, at the stem-cement interface with clinical studies implicating the interface with high failure rates due to ARMD (Bolland et al., 2011; Donell et al., 2010).

Of the tribocorrosion tests of components for THR all are primarily concerned with one part of the entire THR system; the bearing surfaces the taper and the stem-cement interface. Therefore this study considers the role of electrochemical coupling between the stem-cement interfaces and the assumed to be passive Ti-6Al-4V cementless acetabular shell in an attempt to simplify and understand how the system variables interact when subjected to both wear and corrosion. To the authors' knowledge this

study is the first to introduce other interfaces/metals in order understand the role galvanic coupling plays on the corrosion of cemented MoM devices.

2. Experimental Materials and Method

2.1. Test Specimens

In order to gain a full and comprehensive understanding of the role fretting-corrosion and galvanically-enhanced fretting corrosion plays in the overall degradation of cemented femoral stems low carbon (LC CoCrMo) Ultima TPS™ (DePuy International, Leeds, United Kingdom) femoral stems were utilised in this study as the working electrodes (WE). Table 1 gives results from analysis of the Ultima TPS femoral stems along with the ISO 5832-12:2007 standard for the LC alloy.

Table 1 - Chemical composition of alloys tested in this study. † Chemical composition of Ultima TPS™ femoral stem

| | Chemical Composition (% wt) | | | | | | | | | | |
|------------|-----------------------------|------|------|--------|--------|-------|------|------|------|------|------|
| | C | Si | Mn | P | S | Cr | Fe | Mo | N | Ni | Co |
| LC CoCrMo | 0.04 | 0.21 | 0.69 | <0.005 | 0.0008 | 27.65 | 0.41 | 5.40 | 0.17 | 0.48 | Bal. |
| LC CoCrMo† | 0.05 | 0.19 | 0.67 | 0.005 | 0.0010 | 27.65 | 0.30 | 5.48 | 0.18 | 0.24 | Bal. |

In order to replicate the galvanic interaction between the CoCrMo and Ti-6Al-V acetabular components, Ti-6Al-4V rings with the same surface area of the 68mm Ti alloy acetabular component¹ were manufactured. Because it is difficult to estimate the exact surface area of the Ti alloy acetabular component due to the presence of a porous coating, a CAD package (SolidWorks, USA) was utilised to calculate the coated and uncoated area of the acetabular component. A total surface area of 140cm² and 75cm² for the total Ti alloy acetabular cup and porous coated surface area, respectively, was calculated and re-created with the Ti alloy rings (Figure 1). This yields an approximate area ratio of 3:1 for the Ti alloy ring and CoCrMo femoral stem (surface area \approx 58cm²) respectively. Once Ti alloy rings had been manufactured and the Ti-6Al-4V Porocoat® (DePuy International, United Kingdom) porous coating applied, each ring was cleaned and passivated which consisted of ultrasonic cleaning and chemical passivation processes. To facilitate electrochemical measurements a plastic coated Cu wire was glued to

¹ (\varnothing 68mm was the largest Ti-6Al-4V acetabular available on the market at the time and considered to be the worst case scenario with respect to surface area ratios. The entire area of the acetabular cup was assumed to be exposed to the electrolyte. This was informed from clinical retrieval analysis of this particular cohort.)

the surface of the Ti alloy ring and CoCrMo femoral stem using conductive epoxy glue. The junction was then carefully sealed with a impervious sealant to ensure a waterproof connection.

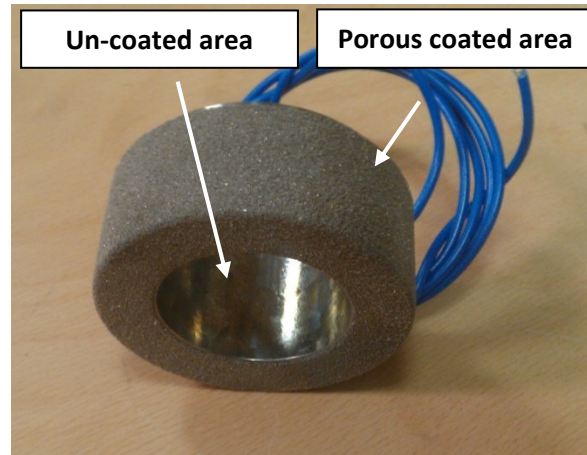


Figure 1 - Ti ring manufactured to represent the acetabular components

The solution used for electrochemical measurements was 0.9% NaCl solution (pH 7.4, 8ppm O₂), prepared using analytical grade reagent and deionised water. Isotonic sodium chloride was used as it has similar ion content to that of the human body fluids, allowing the effects of proteins to be isolated. At this stage the role of protein was neglected due to the complex nature of the electrochemical reactions within the interface and uncertainty as to their interaction at the stem-cement interface. 0.9% NaCl also has a similar Cl⁻ content of the natural synovial fluid.

2.2. Fretting-corrosion Setup

A novel test method was derived, developed and conducted in part reference to ISO 7206-4, to evaluate the mechanically enhanced corrosion mechanisms at the stem-cement interfaces of fully cemented femoral components. Full details of the test arrangement can be found in (Bryant et al., 2013a; Bryant et al., 2013b). Each test was immersed in 600mL of 0.9% NaCl solution at 37±1°C and initially held at a static load of 100N for 24hrs in order to simulate a time of no load bearing after surgery and also to let the system achieve equilibrium before cyclic testing. After 24hrs, a cyclic load of 300N to 2300N at 1Hz for 500,000 cycles was applied to the stem through a Ø28mm LC CoCrMo femoral head and UHMWPE liner. Care was taken to seal the modular taper interfaces to eliminate any additional effects that may result

from corrosion or tribocorrosion processes occurring there. The head and liner interfaces were not immersed to ensure they did not contribute to the electrochemical measurements. Figure 2 demonstrates the test setup and orientation and fixation utilised in this study.

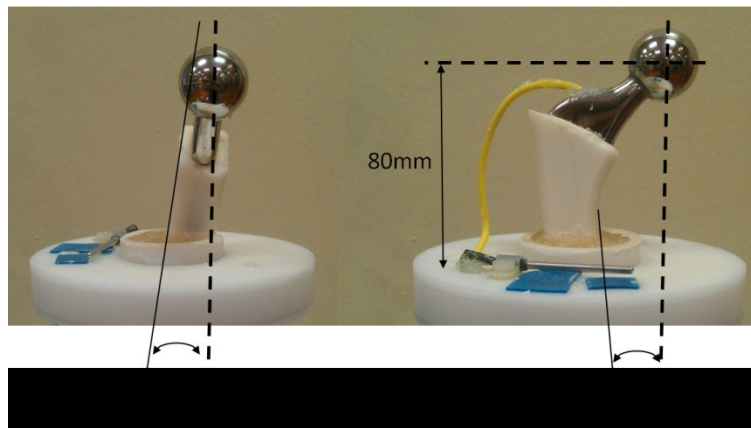


Figure 2 - Orientation and fixation method utilized

2.3. *In-situ* electrochemistry measurements

In order to facilitate *in-situ* corrosion measurements a 3-electrode electrochemical cell was integrated into the ISO 7206-4 fatigue test arrangement. A Thermo-scientific Sureflow Redox combination electrode, consisting of a Ag/AgCl reference electrode (RE) and Pt counter electrode (CE) was employed to facilitate *in-situ* corrosion measurements. In order to quantify the influence of galvanic coupling on the fretting corrosion rates of cemented femoral stems two electrochemical procedures were conducted:

Procedure 1: In order to quantify the free corrosion potential (E_{corr}) and fretting corrosion currents (I_{corr}) of uncoupled cemented femoral stems, intermittent E_{corr} and Linear Polarisation Resistance (LPR) measurements were recorded as a function of time. E_{corr} measurements were conducted every 60secs. Although the LPR technique is considered to be a non-destructive technique, LPR measurements were conducted every 10hrs to minimise disruption of the CoCrMo surface due to polarization. Polarisation scans were conducted from -50mV to +50mV (vs. E_{corr}) at a scan rate of 0.25mV/s. The application of an over-potential to a metallic sample results in a current flow between the WE and CE. Within a small potential range of E_{corr} , a linear relationship between applied potential and measured current is typically seen due to a separation of electrical charge arising from the establishment of the metal oxide and

electrochemical double layer. Above and below E_{corr} , a net anodic or cathodic reaction, respectively, is observed. The slope of the linear polarization curve is related to the kinetic parameters of the corroding system. Experimentally obtained R_p values were inputted into the Stern-Geary (SG) equation using constants obtained from femoral stems subjected to Tafel polarisation whilst undergoing fretting. Tafel polarisation was conducted $\pm 0.5V$ vs E_{corr} . The SG coefficient was calculated as being 0.056. Due to the large number of samples required to obtain Tafel constants as a function of time, the SG coefficient given above was assumed to be constant throughout the test. The authors acknowledge that this assumption is a simplification to the system, but thought to be the most accurate way to determine corrosion currents without extensive polarisation and damage to the surfaces.

It is important to note under this test procedure there is no electrical coupling of the femoral stem to a mixed metal.

Procedure 2: Zero Resistance Ammeter (ZRA) measurements were also utilised in experiments, where there is a galvanic cell set up between the stem-cement interface and Ti ring. The measurements consist of the WE1 and another material (WE2) of interest being connected to a ZRA which allowing a net current to be measured between the two samples. Depending on the convention of current (+ usually anodic, - usually cathodic), the direction of electron flow can be observed. When the net galvanic current (I_g) is equal to zero, no current flows therefore no galvanic corrosion occurs. This does not mean that oxidation of the surfaces is not occurring. This technique only considers the excess corrosion/electron transfer liberated due to fretting-crevice corrosion. It does not take into consideration the current transfer between passive and active areas on the WE. In order to estimate the *actual* corrosion rate ($I_{corr\ galv}$) of the CoCrMo femoral stem when coupled to the Ti alloy ring, other techniques need to be utilised to evaluate the self-corrosion current/rate (current resulting from oxidation and reduction reactions) of the WE (procedure 2). The cell potential (E_{mixed}) of the system was also measured relative to a Ag/AgCl reference electrode. It is important to note that the E_{mixed} reflects the E_{corr} of both the Ti alloy and CoCrMo as both alloys will participate in the redox reactions when electrically coupled.

All electrochemical measurements were conducted using a PGSTAT101 potentiostat/galvanostat (Metrohm Autolab B.V, Utrecht, NL). Figure 3 demonstrates the electrode arrangement for procedures 1 and 2. All results presented in this study represent experimental mean \pm experimental error (n=3).

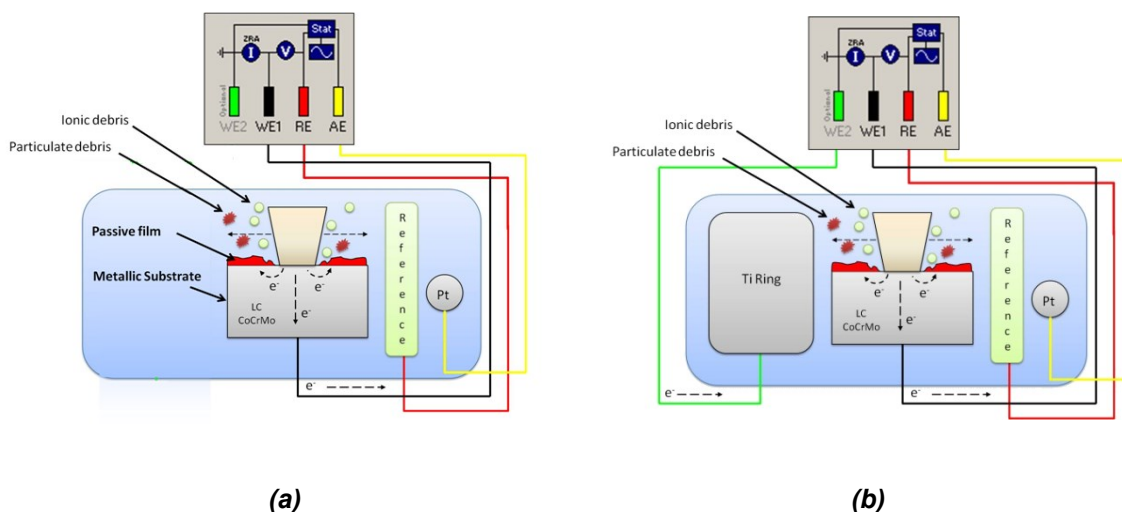


Figure 3 - Schematical representation of the electrode arrangement utilised in a) procedure 1 and b) 2.

Inductively Coupled Plasma-Mass Spectrometry (ICP-MS) tests were conducted to measure the Total Ionic Mass Loss (TIML) during a fretting test. Upon completion of each test 600mL of electrolyte was drained into a sterile polyethylene bottle and stored in the freezer until analysis to prevent further degradation of the solution. Prior to analysis, samples were defrosted and 1mL of bulk electrolyte was extracted using a polymer tipped pipette and stabilised in 9mL 2% HNO_3 . Isotope Co 59, Cr 52, Mo 96 and Fe 58 were used in order to quantify the amount of metal ions released from the metal-cement interface. Cr 52 was chosen to eliminate any interference from Cl (MW: 34.45) and O (MW: 15.99) present in the electrolyte. The combination of ICP-MS and electrochemical techniques highlighted previously allows a mechanistic evaluation of the relative contributions of metallic ions arising from chemical and mechanical degradation. Metallic ion release resulting from chemical dissolution can be further broken down and the influence of galvanic coupling on the pure and wear enhanced-corrosion mechanisms observed.

Low powered optical light microscopy was also conducted in order to assess the surface for any visible areas of fretting-corrosion. Scanning electron microscopy (SEM) was further utilised using a Carl Zeiss EVO MA15 microscope to further elucidate the wear mechanisms acting upon the femoral stems.

3. Results

3.1. *In-situ corrosion measurements*

In order to investigate the role of galvanic coupling under fretting crevice-corrosion conditions Procedures 1 and 2 were conducted. For the galvanic fretting corrosion tests a Ti ring with the same surface area of the acetabular shell in the Ultima THR system was immersed with the femoral stem. Figure 4 demonstrates the cell potential response for both systems. Upon immersion ennoblement in both the E_{corr} and E_{mixed} was seen suggesting the formation of a protective passive oxide/hydroxide layer. At 24hrs this was seen to have stabilised to around 0.08 and 0.11V for the uncoupled and coupled systems respectively.

Upon the application of cyclic loading at 24hrs, a cathodic shift in potential was seen for both the E_{corr} and E_{mixed} was seen respectively. In the case of the uncoupled test, a sudden decrease in E_{corr} is associated with depassivation of the CoCrMo surface and an increase in fretting corrosion current due to exposure of the reactive CoCrMo substrate. For the coupled system, a decrease in E_{mixed} demonstrates depassivation of the CoCrMo surface. The shift in E_{mixed} was not as extreme when compared to E_{corr} values due to the counter effect of cathodic depolarisation imposed on the femoral stem due to the coupling to the Ti alloy ring. This depolarisation also serves to increase the anodic reactions increasing the rate of corrosion. The gradual decrease in E_{mixed} suggests that although depassivation of the CoCrMo occurs upon the application of cyclic loading, the rate of the anodic reaction on the CoCrMo surface, and the areas in which these reactions occur, are in a constant rate of change which will influence the E_{mixed} of the system. Similar trends were seen for all tests.

After 500,000 cycles the cyclic loading was removed and the sample held in compression for a further 10 hrs at 0.3kN. An increase in the E_{corr} and E_{mix} was seen demonstrating a repassivation of the CoCrMo and an ennoblement of the mixed metal system. Throughout the tests an increased cell potential was seen

under both static and fretting conditions when galvanically coupled. This is due to the polarising nature of the Ti alloy ring.

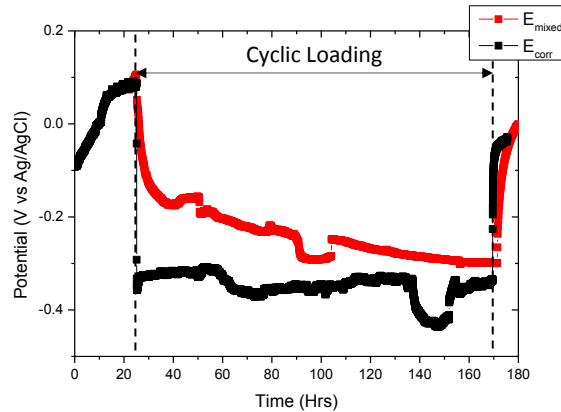


Figure 4 - Measured free corrosion and mixed potential for polished femoral stems when subjected to dynamic loading

Figure 5 demonstrates the fretting-corrosion currents obtained from ZRA and LPR measurements. Upon the application of cyclic loading, I_{corr} was seen to increase by an order of magnitude demonstrating depassivation of the metallic surface and an increase in the rate of oxidation taking place on the metallic surface of the uncoupled system. I_{corr} was seen to remain constant until the removal of load. At this point I_{corr} was seen to decrease suggesting partial repassivation of the CoCrMo and a decrease in the corrosion rate. Furthermore the partial recovery of E_{corr} , combined with the increased I_{corr} compared to the initial static value after cyclic loading had been removed suggests the formation of an environment capable of sustaining an increased rate of localised crevice-corrosion, a characteristic commonly associated with fretting-corrosion of modular head-neck tapers of biomedical implants (Goldberg and Gilbert, 2003).

ZRA measurements demonstrated a net anodic current from the CoCrMo femoral stem to the Ti alloy ring. Upon the application of cyclic loading, on average an increase in current from $7.51 \times 10^{-7} \text{A}$ to $1.75 \times 10^{-5} \text{A}$ was seen demonstrating that galvanic coupling increases the wear-enhanced corrosion. The presence of a galvanic couple significantly increases the rate of pure and wear induced corrosion within the interface.

It is important to realise that net anodic current measurements do not take into consideration any reduction occurring within the stem-cement interface and in the current form are not directly comparable to I_{corr} measurements obtained using the LPR technique. In order to take this into consideration in our galvanic measurements $I_{a(stem)} = I_{corr} + net A$. The effect of this on the fretting-corrosion currents is demonstrated in **Figure 5**. Applying this factor (displayed at $I_{corr}+netA$ in Figure 5), an increase in anodic fretting corrosion current from the CoCr femoral stem was seen. Table 2 summarises the mean currents observed during fretting corrosion tests.

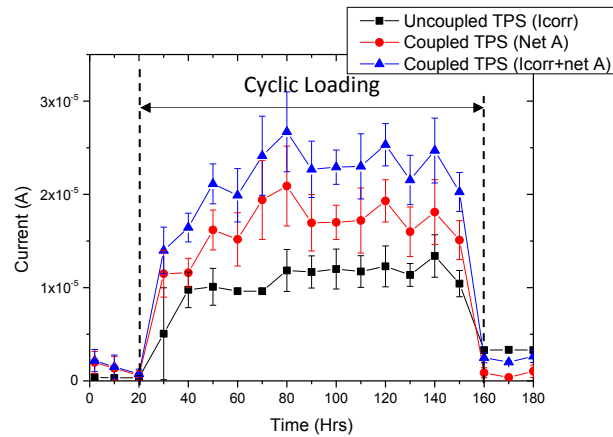


Figure 5 - Current response for uncoupled and coupled polished femoral stems when subjected to dynamic loading

Table 2 – Comparison of mean current during fretting for uncoupled and coupled femoral stems

| | Mean current (A) |
|--|---|
| Uncoupled (I_{corr}) | $1.17 \times 10^{-5} \pm 2.05 \times 10^{-6}$ |
| Coupled (Net A) | $1.64 \times 10^{-5} \pm 2.77 \times 10^{-6}$ |
| Coupled (Net A + I_{corr}) | $2.17 \times 10^{-5} \pm 3.53 \times 10^{-6}$ |

3.2. Ionic Mass Loss

Due to the nature of the system, it is difficult to quantify the total mass loss from the metallic stem gravimetrically due to the formation and accumulation of corrosion product within the cement mantle, along with the removal of the cement mantle in its entirety. Removal of the femoral stem from the PMMA cement will further influence any gravimetric results providing in-accurate and unrepresentative

measurements. The ionic mass loss with respect to time due to pure oxidation and wear induced corrosion of the metallic surface can be calculated from Faraday's relationship shown in equation 1.

$$m = \left(\frac{Q}{F}\right) \times \left(\frac{M}{n}\right) \quad (1)$$

Where 'm' is the ionic mass loss due to pure oxidation and wear induced corrosion of the metallic surface (g), 'Q' is the total electric charge passed through a substance ($Q = \int_0^t I \delta t$, where t is the total time constant, Q=C), $F = 96,485 \text{ C mol}^{-1}$, M is the molar mass of the substance (58.93g assuming stoichiometric dissolution of the alloy) and n is the valence number of ions in the substance (in this case 2 was assuming oxidation according to $\text{Co} \rightarrow \text{Co}^{2+} + 2e^-$). ICP-MS was also utilised to quantify the total ionic mass loss (TIML) in the bulk solution.

Integration of the current vs. time curve was conducted in order to observe the cumulative ionic mass due to chemical dissolution (Figure 6). Galvanic coupling significantly increases the ionic mass loss from 1.39 ± 0.26 to $2.56 \pm 0.31 \text{ mg}$. ICP-MS further supported these findings demonstrating a TIML of 1.44 ± 0.11 and $2.74 \pm 0.19 \text{ mg}$ for uncoupled and coupled femoral stems respectively. Table 3 summarises these findings. An increase in the rate of ionic mass loss due to corrosion $\left(\frac{\partial m}{\partial t}\right)$ from 4.70×10^{-3} to $1.71 \times 10^{-2} \text{ mg hr}^{-1}$ was seen for uncoupled and coupled femoral stems respectively under fretting conditions.

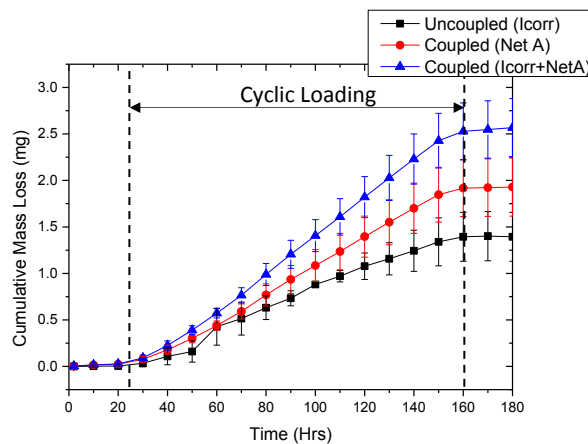


Figure 6- Cumulative ionic mass loss for uncoupled and coupled polished femoral stems when subjected to dynamic loading

Corrosion currents measured with the LPR technique do not take into consideration any ionic/metallic debris liberated from the metallic surface due to mechanical wear; only loss of material by electrochemical corrosion. Any additional metal ions that are produced due to the production and dissolution of debris will therefore be in addition to those measured by electrochemical techniques. ICP-MS provides a good method to do this. The discrepancy between the two measurements will result from the ions which result from the dissolution of any wear debris. Table 3 compares the final ion levels after 500,000 cycles. Corrosion is thought to be the main source of ion release with differences beyond experimental deviation in the TIML and Faradaic mass losses being seen. In all cases Ti was seen to be below the detection limit (<0.50µg/L). This demonstrates that Ti was again acting as the net cathode.

Table 3 – Comparison of Faradaic and Total Ionic Mass Losses.

| | Mass of ions released calculated from Faradays law (mg) | Measured Total Ionic Mass Loss (mg) |
|---|--|--|
| Uncoupled (I_{corr}) | 1.39±0.26 | 1.44±0.11 |
| Coupled (Net A+ I_{corr}) | 2.56±0.31 | 2.74±0.19 |

3.3. Surface Analysis

3.3.1. Macroscopic assessment

Upon the completion of 500,000 cycles, each femoral stem was carefully removed and the surfaces of the CoCrMo femoral stem observed according to the grading and sectioning method present in Figure 7. Upon removal of the uncoupled femoral stem, fretting corrosion could be macroscopically seen in the proximal anterior-lateral and posterior-medial regions of the femoral stem in Gruen zones 1 and 7. Towards the distal regions of the stem, localised areas of pitting corrosion was seen typically in Gruen zone 3. Qualifications for the Gruen Zones can be found in (Bryant et al.; Bryant et al., 2013d)

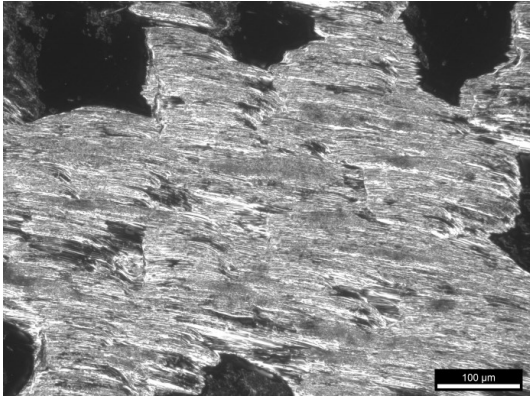


Figure 7 - Location and orientation of Gruen zones used to map fretting corrosion in this study (Bryant et al., 2013d).

3.3.2. Optical Microscopy Images

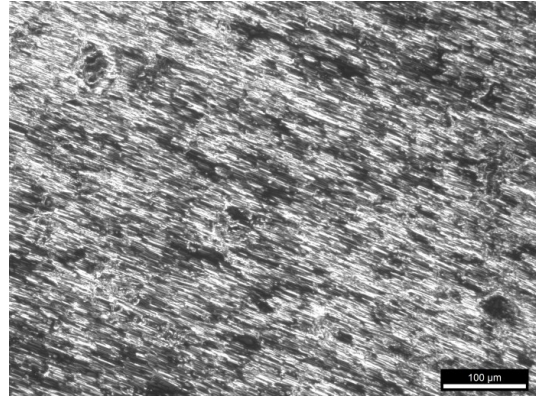
Optical microscope analysis was conducted in order to assess the implications of micro-motion on the surface morphology of cemented femoral stems. A distinct directionality of the surface was seen in the proximal regions of the femoral stem for both uncoupled and coupled CoCr femoral stems (Figure 8a-b). A similar surface morphology was seen in Gruen zones 2,3, 5 and 6 (Figure 8c-d). Localised areas of fretting corrosion were seen to occur around pores found in the counterpart PMMA bone cement, similar to the observation presented by Zhang et al (Zhang et al., 2011). Towards the distal regions of the femoral stems (Gruen zone 4), crevice corrosion was seen in the absence of any micro-motion (Figure 8 e-f).

Uncoupled

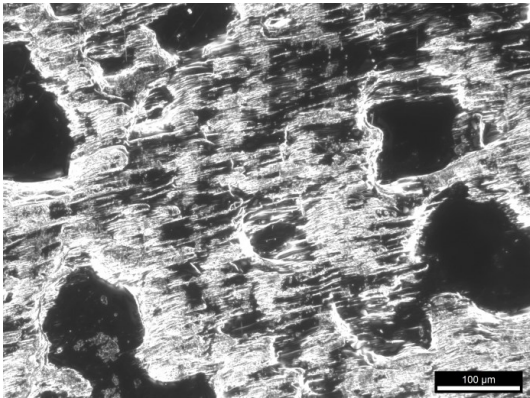


(a)

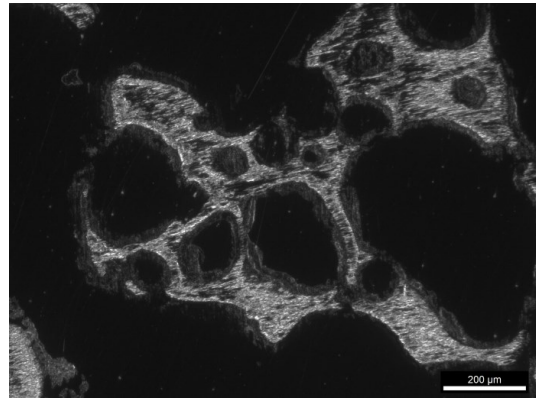
Coupled



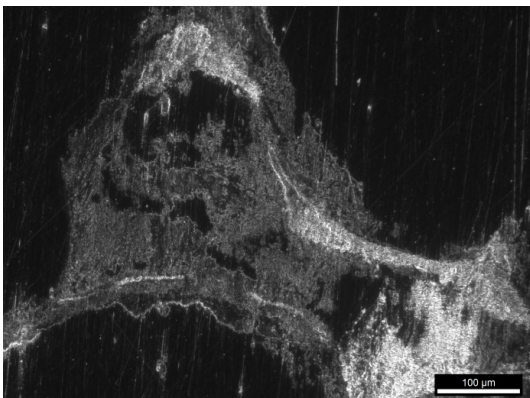
(b)



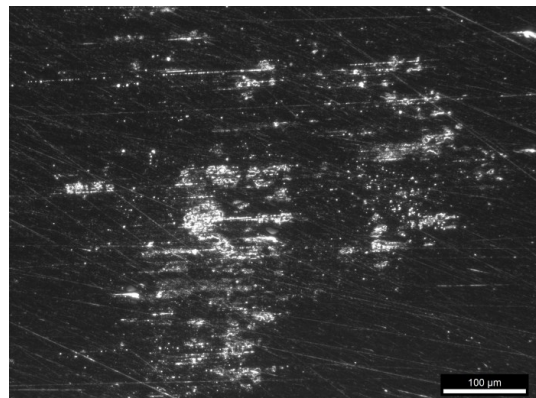
(c)



(d)



(e)



(f)

Figure 8 - Optical Microscope analysis of uncoupled and coupled femoral stems in Gruen zones a-b) 1 and 7 c-d) 2 and 6 e-f) 4

SEM analysis was also conducted on a select number of stems to highlight the difference in surface appearance across the stem-cement interface. As previously mentioned, the mode of degradation was seen to vary as a function of stem length, with a corrosive attack becoming prevalent at the distal portions of the stem. In the regions of which micromotion was present between the CoCr femoral stem and PMMA bone cement an abrasive type wear mechanism could be observed. This was typified by cutting and plough of the CoCr surface.

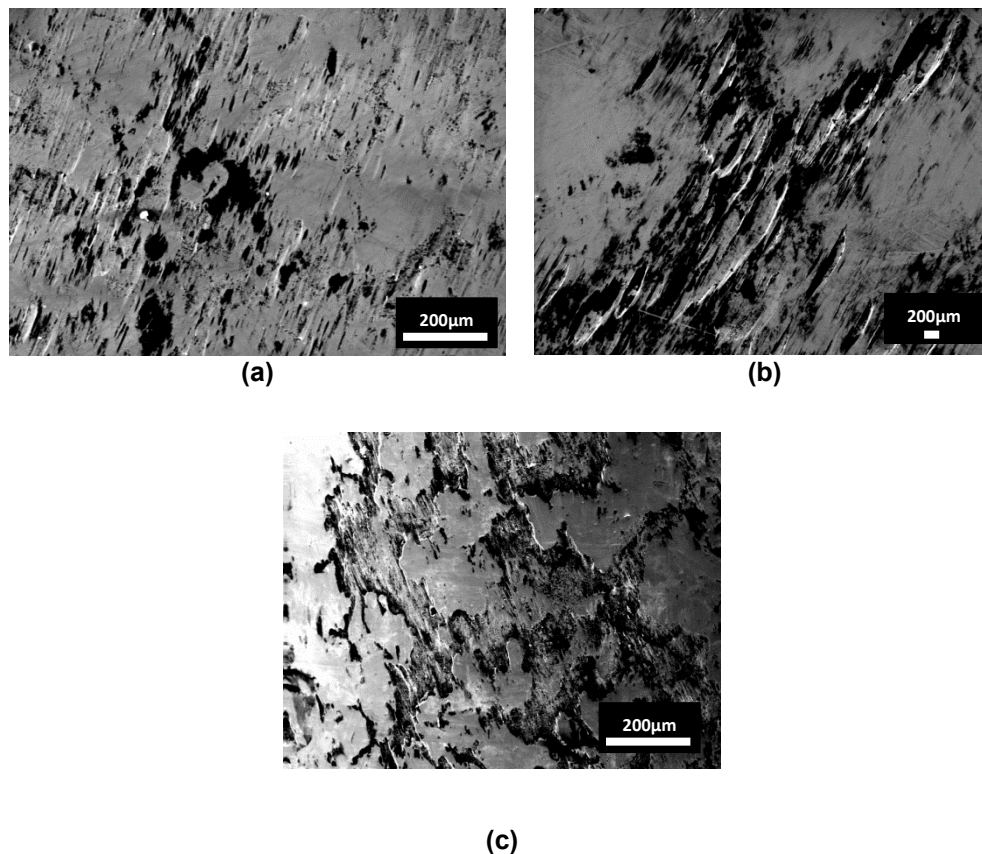


Figure 9 – SE SEM Images of a sample femoral stem in the Gruen Zone a) 1-7 b) 1-7 at higher magnification and c) 4.

4. Discussion

4.1. Tribocorrosion Mechanism

Biomedical alloys typically owe their corrosion resistance to a formation of an inert protective oxide film resulting in very low corrosion rates. In order for a material to form a passive film, the substrate must rapidly react with oxidising agents in the environment (Mischler and Muñoz, 2013). When a passive alloy is utilised in a tribological application, depending on the contact mechanics and lubrication regimes,

mechanical removal of the passive film occurs leaving the reactive substrate exposed to the environment. Rapid oxidation of the substrate usually occurs resulting in metal ions being liberated from the metallic substrate. This process is known as tribocorrosion. Tribocorrosion is found in many engineering applications due the use of lubricating fluid films or the operating environment itself. However the mechanisms involved are not fully understood. Mischler (Mischler et al., 2001) described tribocorrosion as a material deterioration or transformation resulting from simultaneous action of wear and corrosion. The investigation of tribocorrosion requires the control of the chemical conditions during a wear test.

Because tribocorrosion describes both the mechanical removal of material as well as the chemical degradation, it is important to appreciate and to identify the contribution of corrosion and wear to overall material loss. Uhlig, as cited by Mischler (Mischler, 2008), was amongst the first to recognize the role wear and corrosion play on the degradation in fretting contacts. Uhlig demonstrated that material deterioration, and in turn metal ion release, results from two distinct mechanisms; mechanical wear and wear-accelerated corrosion to produce a simple mechanistic model as shown in equation 2, where V_{mech} represents the volume of material removed by mechanical wear, V_{chem} is the material loss due to wear accelerated corrosion.

$$V_{tot} = V_{mech} + V_{chem} \quad (2)$$

In the past the stem-cement interface has been neglected as a primary source of metal ion release only receiving attention from a few researchers. Results from this study have demonstrated that the ion release rates at this interface are not negligible. Studies into the quantity, relative ratios and the exact source of metal ion release from the interfaces of actual biomedical components are rare and limited to MoM bearings. Fretting corrosion currents observed in this study were, if not similar, higher at this interface compared to the articulation surfaces and other modular interfaces demonstrating that the corrosion at this interface is not negligible. Table 4 compares current literature with respect to Faradaic and total mass losses observed in this study.

In reality, MoM THR's are electrically coupled via their interfaces, as well as across the metallic surface, resulting in numerous galvanic cells been established. Currently ISO/ASTM test standards exist outlining

test protocols to investigate the role of wear and corrosion of biomedical devices and materials. However these universally examine one particular component of the implant system in isolation to other system variables and contributors. Galvanic interactions occur when a potential difference is established between two electrically-connected metals immersed in a corrosion or conductive solution, as well areas of passive and depassivated alloy.

Although the mechanisms for fretting corrosion at the stem-cement interface have been explored and reported in literature (Blunt et al., 2009; Brown et al., 2007; Bryant et al., 2013a; Bryant et al., 2013c; Geringer et al., 2005; Geringer and Macdonald, 2012; Geringer et al., 2010; L.Blunt et al., 2009), the role of galvanically-enhanced tribocorrosion and the impact galvanic coupling has on the degradation of orthopaedic implants has not been investigated. Galvanic corrosion is a topic which has been the focus of many discussions in the corrosion science field for many years with mixed findings.

Although the mechanisms of static galvanic corrosion are fairly well understood and thought to be an issue for active-passive and material couples far apart in the galvanic series, galvanic corrosion in the bio-tribocorrosion field is not well understood. Galvanic corrosion of dissimilar metals is one of the most common and most severe forms of corrosion. Mansfeld (Mansfeld, 1973) highlighted that the magnitude of galvanic corrosion depends not only on the potential differences of mixed metals, but also on kinetic parameters such as corrosion rates or exchange current densities of the uncoupled materials. Papageorgio and Mischler (Papageorgiou and Mischler, 2012) have recently highlighted the importance and implications of galvanic coupling between active and passive regions found on a material when subjected to tribological conditions (i.e. potential difference established inside and outside the wear track), modelling potential and current transients based upon the Tafel equation. This potential difference between the active wear track and passive surrounding areas results in an electron flow, resulting in accelerated corrosion of the more susceptible alloy (Anode) and protection of the other areas (Cathode).

Apply these current concepts and understandings, galvanic interactions between the passive and active areas on the CoCr femoral stem are expected during fretting, giving rise to the characteristic E_{corr} curve presented in Figure 4. The electrochemical reactions occurring at the stem-cement interface can be visualised using Evans' diagrams. Figure 10 represents the evolution of current of the cathodic and

anodic reactions for the uncoupled and coupled situations. E_{corr1} corresponds to the intersect at which the rate of the anodic reactions is equal to the cathodic reaction in the absence of fretting. At this point the self-corrosion rate at the interface is established (I_{corr1}). Upon the application of fretting, an increase in the rate of metal oxidation is seen due to the loss of passivity resulting in a negative shift in E_{corr1} to E_{corr2} and an increase in the rate of corrosion to I_{corr2} . Mischler and Munoz (Mischler and Muñoz, 2013) have highlighted that since the depassivated and still passive areas are in electronal contact, a galvanic coupling occurs between active and passive areas on the alloy.

For the case where passive Ti alloy is electrically connected to the stem-cement interface, a second galvanic couple or redox reaction is introduced. According to mixed potential theory, because we have an additional reduction reaction (O_2 reduction on Ti-6Al-4V) and assuming the dissolution of Ti alloy is negligible, the rate of the reduction and oxidation reactions need to be equal to satisfy charge conservation. In addition to this, as two electron consumption reactions are present these need to be summed giving rise to the qualification presented above. This therefore results in an increase in the rate of corrosion and release of metal ions into the bulk solution as demonstrated in Figure 10b.

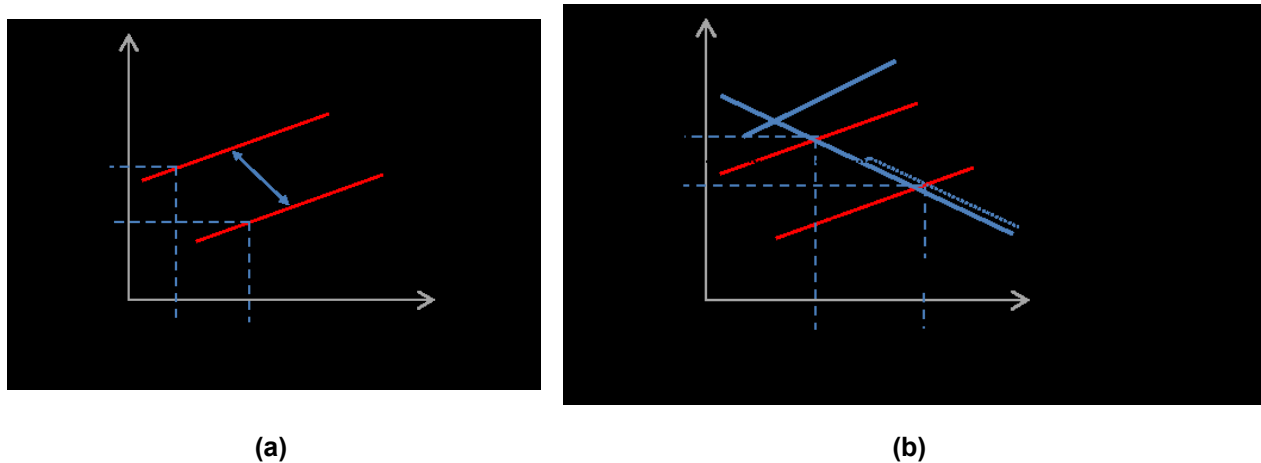


Figure 10 - Simplified Evans diagrams demonstrating the mechanisms for potential and current shifts for a) uncoupled and b) femoral stems coupled to Ti-6Al-4V.

The results presented in this study support this hypothesis and demonstrate that the presence of static and passive Ti alloys and other metals will anodically polarise the CoCrMo femoral stem, increasing the rate of oxidation within the interface due to the large potential differences established between the

passive Ti alloy ring and fretting contact. This is not surprising and has been shown by many authors (Guadalupe Maldonado et al., 2013; Landolt et al., 2001; Stack and Chi, 2003) that by increasing the over-potential of a system, wear-corrosion transitions can be observed depending the nature of the alloy. This paper highlights the need and importance of developing and taking a systems approach (i.e. understanding the interactions between other components rather than studying them in isolation) when considering the degradation mechanisms of orthopaedic alloys. Electrochemical reactions occurring across other interfaces have the ability to accelerate or suppress the dissolution mechanisms at localised interfaces. This will have a drastic effect on the overall performance of the construct which will not be captured when interfaces are studied in isolation.

4.2. *Wear Mechanism*

Surfaces demonstrated a characteristic surface morphology depending of the degradation mechanism acting on them. Howell *et al* (Howell et al., 2004a; Howell et al., 2004b) presented a comprehensive study, conducting SEM and 3-D interferometry analysis on both retrieved polished and matte femoral stems. Polished stems were seen to exhibit signs of ductile wear accompanied by pitting of the surface typically in the anterolateral and posteromedial aspects of the stem, similar to the locations of wear and corrosion observed in this study. SEM analysis presented in this study (Figure 9) demonstrates cutting and plastic deformation of the CoCr femoral surface suggesting the presences of an abrasive wear mechanism. An abrasive wear mechanism exists at the stem-cement interface due to the formation and transfer of a Cr_2O_3 particulate film. Subsequently a hardness differential between the femoral stem (5-10GPa) and Cr_2O_3 film (14-30GPa) will be established, resulting in abrasion of the femoral stem and depassivation of the surface. Evidence has been presented in previous studies (Figure 11) which has demonstrated the formation and presence of Cr_2O_3 films in the stem cement interface, creating a third body abrasive wear scenario. This was also seen to be of similar composition of that observed in retrieval studies.

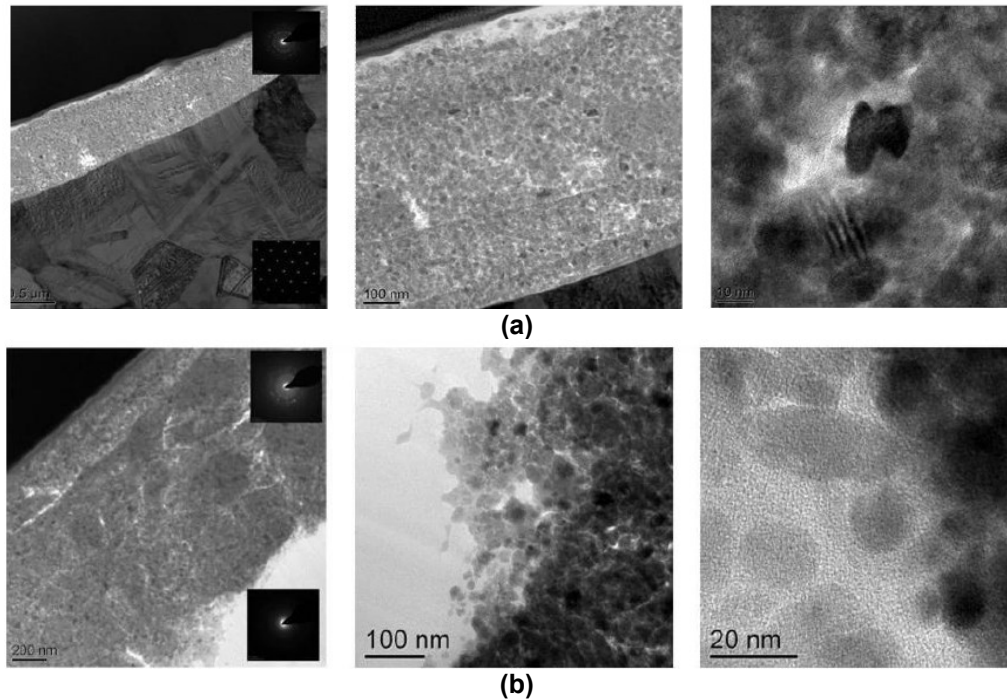


Figure 11 - Fretting corrosion product found on a) stem and b) PMMA bone cement after 500,000 cycles of fretting (Bryant et al., 2013b).

4.3. Links to Clinical Data

In 2008, Donell et al (Donell et al., 2010) reported the dramatic corrosion of generally solidly fixed femoral stems when combined with MoM articulations. The current revision rate stands at 20.2% at 15 years post-op (Bryant et al., 2013d). It was thought that the necrosis of the surrounding tissue was associated with the release of potentially toxic metal ions such as cobalt and chromium from the stem-cement interface due to corrosion of the alloy. In contrast to this, Shetty *et al* (Shetty et al., 2006; Shetty et al., 2005) presented the findings of the Ultima TPS femoral stem when used in conjunction with a MoP articulation. No hips required revision within 5 years due to ARMD when used in conjunction with a MoP articulation and 'a similar performance as the Exeter femoral stem' which has at least 20 years of clinical prevalence was seen. Although anecdotal, this suggests an effect of the MoM articulation on corrosion mechanisms and rates at the stem-cement. A subsequent publication by Bolland *et al* (Bolland et al., 2011) further demonstrated high levels of corrosion of the cemented portions of the femoral stem in a same-metal MoM system further supporting this hypothesis.

Tribo-chemical reactions have also been shown to be a predominant factor in the degradation at the stem-cement-interface of MoM THR influencing the ratios in which metallic ions were released at the stem-cement interface. Previous publications have demonstrated that the formation of films within the interface significantly influences the ion release from the interface due to the thermodynamic stability of the alloying elements within the interface (Bryant et al., 2013a; Bryant et al.; Bryant et al., 2013d). To date there are no reported *in-vitro* studies of direct measurements of ionic mass loss from the stem-cement interface into the bulk environment. Hart *et al* (Hart et al., 2013) presented the tissue findings of the Ultima TPS MoM cohort which are in good agreement with the experimental findings demonstrating a preferential release of Co into the biological environments. This is due to the formation of chromium rich oxide layers being formed within in the stem-cement interface as a result of fretting, resulting in a preferential release of Co. These findings also further question the use of *in-vivo* metal ion measurements as a surrogate marker of wear in MoM total hip replacements as the tribochemical reactions occurring at these interfaces have the propensity to influence the actual metal ions released in the biological environment.

Table 4- Comparison of electrochemical parameters ionic mass losses from recent in-vivo studies on orthopaedic components

| Study | Interface Observed | Electrochemical Technique | Max. observed I_{corr} / change in cell potential under depassivation | Faradaic / Total Ionic Mass Loss (mg) (Ratio Co:Cr:Mo) | Duration of Test | Test Electrolyte |
|---|----------------------------|---------------------------|---|--|--------------------------------|---|
| This Study | Stem-Cement | LPR/ZRA/ E_{corr} | Uncoupled: $3.5 \times 10^{-6}A/$ $\Delta 0.24V$ | Uncoupled: 0.91/1.49 (9.5:0.3:0.2) | 0.5million cycles | 0.9% NaCl |
| | | | Coupled: $2.5 \times 10^{-5}A/$ $\Delta 0.36V$ | Coupled: 2.54/2.73 (9.8:0.1:0.1) | | |
| Hesketh et al (Hesketh et al., 2013) | 36mm MoM Articulation | LPR/ E_{corr} | $6.0 \times 10^{-6}A/$ $\Delta 0.35V$ | 0.535/1.1 (6:3:1) | 1million cycles | 18g/l foetal bovine serum diluted with PBS and 0.03% sodium azide |
| Al-Hajjar et al (Al-Hajjar et al., 2013) | 28 & 36mm MoM Articulation | - | - | NA/0.22-1.12 | Correlated against wear volume | 25% (v/v) calf serum with 0.03% sodium azide |
| Heisel et al (Heisel et al., 2008) | 47mm MoM resurfacings | - | - | NA/ $\approx 10000\mu g/L$ (6.5:2.8:0.7) | 3million cycles | 30g/L Serum content |
| Goldberg et al (Goldberg and Gilbert, 2003) | Head neck taper | ZRA | $7.2 \times 10^{-6}A/$ $\Delta 0.35V$ | NA/ max. 0.03 | 1million cycles | Phosphate Buffered Saline (PBS) |

This study highlights the importance of the galvanic coupling of the Ti alloy shell in the Ultima TPS system to the stem-cement interface with respect to the occurrence and magnitude of galvanic corrosion. These results demonstrate that consideration must be taken when designing and researching biomedical devices and that there is a need for new generation of test techniques and simulation methods that would accommodate such factors. Further work also needs to be conducted to understand the potentials established across the surface of metals and mixed metal systems as well as the influence of surface area ratios.

5. Conclusions

Electrochemical techniques combined with visual, optical, electron microscopy and solution chemistry techniques have been utilised in order to identify the role of galvanic coupling on the fretting-corrosion rates and metallic ion production of cemented polished femoral stems. From this study it can be concluded that:

- The introduction of cyclic loading results in a depassivation of the CoCrMo femoral stem surface.
- The presence of Ti significantly increases the rate of wear enhance oxidation increasing the rate in which metal ions are produced.
- A 100% increase in total ion release was seen for femoral stems coupled to Ti.
- Large potential differences between the Ti alloy and active CoCrMo surface are established due to depassivation of the femoral stem surface resulting in a large current flow from the CoCrMo surface to the Ti.
- Ti alloy increases the rate of wear enhanced oxidation by polarising the femoral stem surface according to the mixed potential theory.
- A corrosive wear mechanism is seen at the stem-cement interface, with corrosion accounting for 95% of all metal ions released for uncoupled and coupled femoral stems respectively.

References

- A.Santavirta, M.Bohler, W.Harris, 2003. Alternative materials to improve total hip replacement tribology. Acta Orthop Scand 74, 380-388.
- Al-Hajjar, M., Fisher, J., Williams, S., Tipper, J., Jennings, L., 2013. Effect of femoral head size on the wear of metal on metal bearings in total hip replacements under adverse edge-loading conditions. J Biomed Mater Res Part B 101, 213-222.
- Blunt, L.A., Zhang, H., Barrans, S.M., Jiang, X., Brown, L.T., 2009. What results in fretting wear on polished femoral stems. Tribology International 42, 1605-1614.
- Bolland, B.J.R.F., Culliford, D.J., Langton, D.J., Millington, J.P.S., Arden, N.K., Latham, J.M., 2011. High failure rates with a large-diameter hybrid metal-on-metal total hip replacement: CLINICAL, RADIOLOGICAL AND RETRIEVAL ANALYSIS. Journal of Bone & Joint Surgery, British Volume 93-B, 608-615.
- Brown, L., Zhang, H., Blunt, L., Barrans, S., 2007. Reproduction of fretting wear at the stem-cement interface in total hip replacement. Proceedings of the Institution of Mechanical Engineers.Part H, Journal of engineering in medicine 221, Nov.
- Bryant, M., Farrar, R., Brummitt, K., Freeman, R., Neville, A., 2013a. Fretting corrosion of fully cemented polished collarless tapered stems: The influence of PMMA bone cement. Wear 301, 290-299.
- Bryant, M., Farrar, R., Freeman, R., Brummitt, K., Neville, A., 2013b. Fretting Corrosion Characteristics of Polished Collarless Tapered Stems in a Simulated Biological Environment. Tribology International.
- Bryant, M., Farrar, R., Freeman, R., Brummitt, K., Neville, A., 2013c. Fretting corrosion characteristics of polished collarless tapered stems in a simulated biological environment. Tribology International 65, 105-112.
- Bryant, M., Ward, M., Farrar, R., Freeman, R., Brummitt, K., Nolan, J., Neville, A., Characterisation of the surface topography, tomography and chemistry of fretting corrosion product found on retrieved polished femoral stems. Journal of the Mechanical Behavior of Biomedical Materials.
- Bryant, M., Ward, M., Farrar, R., Freeman, R., Brummitt, K., Nolan, J., Neville, A., 2013d. Failure analysis of cemented metal-on-metal total hip replacements from a single centre cohort. Wear 301, 226-233.
- Burston, J., Barnett, J., Amirfeyz, R., Yates, R., Bannister, G., 2012. Clinical and radiological results of the collarless polished tapered stem at 15 years follow-up. The Journal of Bone and Joint Surgery [Br] 94.
- Donell, S.T., Darrach, C., Nolan, J.F., Wimhurst, J., Toms, A., Barker, T.H.W., Case, C.P., Tucker, J.K., Group, N.M.-o.-M.S., 2010. Early failure of the Ultima metal-on-metal total hip replacement in the presence of normal plain radiographs. Journal of Bone & Joint Surgery, British Volume 92-B, 1501-1508.
- Fisher, J.B.P.D., Jin, Z.B.P., Tipper, J.B.P., Stone, M.M.M.F., Ingham, E.B.P., 2006. PRESIDENTIAL GUEST LECTURE: Tribology of Alternative Bearings. Clinical Orthopaedics & Related Research December 453, 25-34.
- Geringer, J., Forest, B., Combrade, P., 2005. Fretting-corrosion of materials used as orthopaedic implants. Wear, 943-951.
- Geringer, J., Macdonald, D.D., 2012. Modeling fretting-corrosion wear of 316L SS against poly(methyl methacrylate) with the Point Defect Model: Fundamental theory, assessment, and outlook. Electrochimica Acta 79, 17-30.
- Geringer, J., Normand, B., Alemany-Dumont, C., Diemiaszonek, R., 2010. Assessing the tribocorrosion behaviour of Cu and Al by electrochemical impedance spectroscopy. Tribology International 43, 1991-1999.
- Goldberg, L., Gilbert, J., 2003. ***In Vitro Corrosion Testing of Modular Hip Tapers***. J Biomed Mater Res Part B 64B, 79-93.

Guadalupe Maldonado, S., Mischler, S., Cantoni, M., Chitty, W.-J., Falcand, C., Hertz, D., 2013. Mechanical and chemical mechanisms in the tribocorrosion of a Stellite type alloy. *Wear* 308, 213-221.

Hart, A.J., Quinn, P.D., Lali, F., Sampson, B., Skinner, J.A., Powell, J.J., Nolan, J., Tucker, K., Donell, S., Flanagan, A., Mosselmans, J.F.W., 2013. Cobalt from metal-on-metal hip replacements may be the clinically relevant active agent responsible for periprosthetic tissue reactions. *Acta Biomaterialia* 8, 3865-3873.

Heisel, C., Striech, N., Krachler, M., Jaubowitz, E., Kretzer, P., 2008. Characterization of the running-in period in total hip resurfacing arthroplasty: An in vivo and in vitro metal ion analysis. *J Bone Joint Surg Am* 90, 125-133.

Hesketh, J., M, Q., Dowson, D., Neville, A., 2013. Biotribocorrosion of metal-on-metal hip replacements: How surface degradation can influence metal ion formation. *Tribology International*.

Howell, J.R., Blunt, L., Doyle, C., Hooper, R.M., Lee, A.J., Ling, R.S., 2004a. ***In Vivo Surface Wear Mechanisms of Femoral Components of Cemented Total Hip Arthroplasties***. *The Journal of Arthroplasty* 19.

Howell, J.R., Blunt, L.A., Doyle, C., Hooper, R.M., Lee, A.J.C., Ling, R.S.M., 2004b. In Vivo surface wear mechanisms of femoral components of cemented total hip arthroplasties: the influence of wear mechanism on clinical outcome. *The Journal of Arthroplasty* 19, 88-101.

Jacobs, J.J., Skipor, A.K., Patterson, L.M., Hallab, N.J., Paprosky, W.G., Black, J., Galante, J.O., 1998. Metal release in patients who have had a primary total hip arthroplasty. A prospective, controlled, longitudinal study. *Journal of Bone & Joint Surgery - American Volume* 80, 1447-1458.

L.Blunt, H.Zhang, S.Barrans, X.Jiang, L.Brown, 2009. What results in fretting wear on polished femoral stems. *Tribology International* 42, 1605-1614.

Landolt, D., Mischler, S., Stemp, M., 2001. Electrochemical methods in tribocorrosion: a critical appraisal. *Electrochimica Acta* 46, 3913-3929.

Mansfeld, F., 1973. The Relationship Between Galvanic Current and Dissolution Rates. *Corrosion* 29, 403-405.

Mischler, S., 2008. Triboelectrochemical techniques and interpretation methods in tribocorrosion: A comparative evaluation. *Tribology International* 41, 573-583.

Mischler, S., Muñoz, A.I., 2013. Wear of CoCrMo alloys used in metal-on-metal hip joints: A tribocorrosion appraisal. *Wear* 297, 1081-1094.

Mischler, S., Spiegel, A., Stemp, M., Landolt, D., 2001. Influence of passivity on the tribocorrosion of carbon steel in aqueous solutions. *Wear* 251, 1295-1307.

National Joint Registry, 2012. National Joint Registry for England and Wales: 9th Annual Report 2012, <http://www.njrcentre.org.uk/NjrCentre/LinkClick.aspx?fileticket=QkPI7kk6B2E%3d&tabid=86&mid=52>.

Papageorgiou, N., Mischler, S., 2012. Electrochemical Simulation of the Current and Potential Response in Sliding Tribocorrosion. *Tribology Letters* 48, 271-283.

Purbach, B., Kay, P., Wroblewski, M., Siney, P., Flemming, P., 2009. Triple tapered cemented polished stem in total hip arthroplasty. A review of 1008 cases using the c-stem with a minimum of 5 years clinical and radiological follow-up. *The Journal of Bone and Joint Surgery [Br]* 91-B.

Reynolds, L.A., Tansey, E.M., 2006. EARLY DEVELOPMENT OF TOTAL HIP REPLACEMENT, 1 ed. Wellcome Trust Centre, London, UK.

Shetty, N., Hamer, A., Kerry, R., Stockley, I., Eastell, R., Wilkinson, J., 2006. Exeter versus Ultima-TPS femoral stem: a randomised early outcomes study. *The Journal of Bone and Joint Surgery [Br]* 88-B.

Shetty, N., Hamer, A., Stockley, I., Eastell, R., Wilkinson, J., 2005. Clinical and radiological outcome of total hip replacement five years after pamidronate therapy. *The Journal of Bone and Joint Surgery [Br]* 88-B, 889.

Stack, M.M., Chi, K., 2003. Mapping sliding wear of steels in aqueous conditions, *Wear* 14th International Conference on Wear of Materials, pp. 456-465.

World Health Organisation, 2003. Musculoskeletal conditions affect millions, Corrosion Science.

Zhang, H., Brown, L., Blunt, L., Jiang, X., Barrans, S., 2011. The contribution of the micropores in bone cement surface to generation of femoral stem wear in total hip replacement. Tribology International 44, 1476-1482.

LIST OF FIGURES

Figure 4 - Ti ring manufactured to represent the acetabular components

Figure 5 - Orientation and fixation method utilized

Figure 6 - Schematical representation of the electrode arrangement utilised in a) procedure 1 and b) 2.

Figure 4 - Measured free corrosion and mixed potential for polished femoral stems when subjected to dynamic loading

Figure 5 - Current response for uncoupled and coupled polished femoral stems when subjected to dynamic loading

Figure 6- Cumulative ionic mass loss for uncoupled and coupled polished femoral stems when subjected to dynamic loading

Figure 7 - Location and orientation of Gruen zones used to map fretting corrosion in this study (Bryant et al., 2013d).

Figure 8 - Optical Microscope analysis of uncoupled and coupled femoral stems in Gruen zones a-b) 1 and 7 c-d) 2 and 6 e-f) 4

Figure 9 – SE SEM Images of a sample femoral stem in the Gruen Zone a) 1-7 b) 1-7 at higher magnification and c) 4.

Figure 10 - Simplified Evans diagrams demonstrating the mechanisms for potential and current shifts for a) uncoupled and b) femoral stems coupled to Ti-6Al-4V.

Figure 11 - Fretting corrosion product found on a) stem and b) PMMA bone cement after 500,000 cycles of fretting (Bryant et al., 2013b).

LIST OF TABLES

Table 2 - Chemical composition of alloys tested in this study. † Chemical composition of Ultima TPS™ femoral stem

Table 2 – Comparison of mean current during fretting for uncoupled and coupled femoral stems

Table 3 – Comparison of Faradaic and Total Ionic Mass Losses.

Table 4- Comparison of electrochemical parameters ionic mass losses from recent in-vivo studies on orthopaedic components